PROCEEDINGS OF SPIE
SPIE—The International Society for Optical Engineering

Photon Management

Frank Wyrowski
Chair/Editor

27–28 April 2004
Strasbourg, France

Sponsored and Published by
SPIE—The International Society for Optical Engineering

Cooperating Organizations
EOS—European Optical Society (United Kingdom)
SFO—Société Française d'Optique (France)
SIOF—Società italiana di Ottica e Fotonica (Italy)
DGaO—Deutsche Gesellschaft für angewandte Optik (Germany)
IEE—The Institution of Electrical Engineers
Photonics Clusters (United Kingdom)
oe*magazine*
NEMO—Network of Excellence in Micro-Optics

Supported by
Région Alsace (France)
Communauté Urbaine de Strasbourg (France)
Conseil Général du Bas-Rhin (France)
Alsace Development Agency (France)
European Office of Aerospace Research and Development,
U.S. Air Force Office of Scientific Research

Volume 5456

The papers included in this volume were part of the technical conference cited on the cover and title page. Papers were selected and subject to review by the editors and conference program committee. Some conference presentations may not be available for publication. The papers published in these proceedings reflect the work and thoughts of the authors and are published herein as submitted. The publisher is not responsible for the validity of the information or for any outcomes resulting from reliance thereon.

Please use the following format to cite material from this book:

Author(s), "Title of Paper," in *Photon Management*, edited by Frank Wyrowski, Proceedings of SPIE Vol. 5456 (SPIE, Bellingham, WA, 2004) page numbers.

ISSN 0277-786X
ISBN 0-8194-5383-8

Published by
SPIE—The International Society for Optical Engineering
P.O. Box 10, Bellingham, Washington 98227-0010 USA
Telephone 1 360/676-3290 (Pacific Time)· Fax 1 360/647-1445
http://www.spie.org

Printed in the United States of America.

Depth attenuated refractive index profiles in holographic gratings recorded in photopolymer materials

S. Gallego*[a], M. Ortuño[a], C. Neipp[b], A. Márquez[b], J.T. Sheridan[c], A. Beléndez[b] and I. Pascual[a]

[a]Departamento Interuniversitario de Óptica, Universidad de Alicante, Ap. 99, Alicante, Spain E-03080;
[b]Departamento de Física, Ingeniería de Sistemas y Teoría de la Señal, Universidad de Alicante Ap. 99, Alicante, Spain E-03080;
[c]Departament of Electronic and Electrical Engineering, University College Dublin, Belfield, Dublin 4, Republic of Ireland

ABSTRACT

Photopolymers are systems of organic molecules that rely on photoinitiated polymerization to record volume phase holograms. Characteristics such as good light sensitivity, large dynamic range, good optical properties and relatively low cost make photopolymers one of the most promising materials for write-one, read-many (WORM) holographic data storage applications. Thus, it is interesting to understand the mechanisms that control the way information is stored in photopolymer materials. Different authors have demonstrated that two processes play the main role in hologram formation: monomer polymerization and monomer diffusion. A number of models based on these two processes have been proposed and their prediction capability has been validated. In this work we extend the capabilities of the existent models by introducing another important characteristic: the attenuation of light through the depth of the material which happens in the recording process. In order to check the validity of the theoretical model that we propose, volume phase transmission gratings are recorded in a PVA/Acrylamide photopolymer with different spatial frequencies. Using the Rigorous Coupled Wave Theory (RCWT) we show that we can obtain information about the higher harmonics in the recorded refractive index modulation. Comparison between simulated and experimental results validates the interpretation provided by the proposed model.

Keywords: Holography; Volume gratings, Holographic recording materials, Photopolymers

1. INTRODUCTION

Photopolymers are attractive materials for the production of high quality holograms[1-3]. This material presents some well-known advantages, such as the possibility of obtaining high efficiencies (up to 100%), high thickness (to use as holographic data storage medium) and relativity low cost. Photopolymer systems for recording holograms typically comprise one or more monomers, a photoinitiation system and an inactive component often referred to as a binder. Other components are sometimes added to control a variety of properties such as sensitivity and viscosity of the recording medium. Although complex, the mechanism of hologram formation is assumed to be a consequence of the interplay between the processes of monomer polymerization and monomer diffusion, which take place when the material is illuminated. Recently, several models taking into account these two processes have been used to describe the mechanism of hologram formation inside photopolymer materials[4-15]. It is the first model proposed by Zhao et al.[5] which provided the basis for polymerization driven diffusion (PDD) models of hologram formation in photopolymers. Although the model proposed by Zhao et al. predicted the general behaviour of photopolymerization when diffraction gratings are recorded in photopolymer materials, it failed to explain the cut-off of the diffraction efficiency for high

* cristian@dfists.ua.es; phone: +34-96-5903651; Fax: +34-96-5909750

spatial frequencies. This was successfully achieved by Sheridan and co-workers, who implemented a non-local polymerization driven diffusion (NPDD)[11-13]. The main feature of this model is that it includes a non-local response function that takes into account the growth of polymer chains inside the photopolymer material. The model has also the particularity that for the limiting case in which the non-local effects are disregarded the model reduces exactly to the PDD proposed by Zhao et al.

Another feature shared by some models is that the polymerization rate, that is the rate of conversion of monomer in polymer by photopolymerization, has a linear dependence to the intensity pattern stored in the photopolymer material. Although, it has been recently demonstrated that it is more accurate to assume a non-linear dependence[9,13,14]. In general, it can be said that a great work has been done in the field of theoretical models that explain the mechanism of hologram formation in photopolymers. Nonetheless, in spite of the great progress that has been made in this field, there are still some lacks in the theoretical models to aproppiatedly predict the general behavior of these materials. One of the features that the models have not explained yet, is the attenuation of the refractive index profile inside photopolymer materials of high thickness. This attenuation is due to absorption of light by the Dye existing in the material when this is illuminated, attenuation which is caused by the Beer's law. Although this law has been taken into account in some models, such as some works published by Blaya et al.[16,17], the attenuation effect through the depth of the material has not been treated.

In this work we will demonstrate that a polymerization mechanism creates a non-uniform monomer and polymer concentration through the depth of the hologram. The main effect of this non-uniformity is to create an attenuated profile of the refractive index through the hologram. To incorporate this effect in the RCW formalism we developed a method[18] based on the implemented RCW approach proposed by Moharam et al.[19]. Using the algorithm we propose[18], the efficiencies of the different orders that propagate inside the hologram are calculated for a theoretical transmission diffraction grating of 540 lines/mm. It will be shown that the main effect of an attenuated refractive index profile is to smooth the off-Bragg curves of the efficiencies of the different orders. The theoretical model proposed will be also tested by comparing its predictions to experimental data obtained in holographic gratings recorded in photopolymer materials.

2. MODEL OF PHOTOPOLYMERIZATION AND ATTENUATION OF MONOMER AND POLYMER CONCENTRATIONS

In this section we will introduce a general model of photopolimerization to demonstrate that the effect of light absorption by the material is to attenuate the monomer and polymer concentration in depth. The model as is presented here is due to Terrones and Pearlstein[20].

The mechanism of photopolymerization can be described in terms of the following processes:

1) Firtsly, light is absorbed by a photoiniator A to create radicals R•

$$A \xrightarrow{h\nu} fR^{\bullet} \tag{1}$$

2) The free radicals bind to monomer to form the chain-initiation species

$$R^{\bullet} + M \xrightarrow{k_p} RM^{\bullet} \tag{2}$$

3) The radical RM• propagates forming macroradicals

$$RM_m^{\bullet} + M \xrightarrow{k_p} RM_{m+1}^{\bullet} \quad m \geq 1 \tag{3}$$

4) Finally, two macroradicals combine to form a polymer chain

$$RM_m^{\bullet} + RM_n^{\bullet} \xrightarrow{k_{t,m,n}} RM_{m+n}R \quad m,n \geq 0 \tag{4}$$

In the steady-state approximation for radical concentrations, the chemical equations derived by Terrones and Pearlstein that describe the polymerization mechanism are[20]:

$$\frac{\partial[A]}{\partial t} = -\phi\alpha_A I(z,t)[A] \tag{5}$$

$$I(z,t) = I_0 \exp\left[-\alpha_A \int_0^z [A(z',t')]dz'\right] \tag{6}$$

$$\frac{\partial[M]}{\partial t} = -k_p\sqrt{f\phi\alpha_A I(z,t)[A]/k_t}[M] \tag{7}$$

α_A is the absorption coeeficient, [A] and [M] the molar concentration of photoinitiatior and monomer, respectively, ϕ is the quantum yield of initiator consumption. I_0 is the incident light intensity, f accounts for the possibility that the initiator gives rise to one or two primary radicals and k_p and k_t are the propagation and termination rate constants respectively. The variable z indicates variation through the depth of the material. It is important to note that the intensity has not x,y variation. Thus, we assume that no interference pattern is recorded in the material, since at this stage we are only interested in generally describing how absorption of light influences on the variation in depth of the monomer and polymer concentration. In a further step we will introduce these effects in the NPDD models.

Equation (6) takes into account Beer's law whereas equations (5) and (7) described the variation in time of the photoinitiator and monomer concentration, respectively.

The initial conditions for equations (5) and (7) are:

$$[A(z,0)]=[A]_0$$
$$[M(z,0)]=[M]_0$$

The solutions of equations (5) and (7) with the aforementioned initial conditions are:

$$[A_N] = \left[1 + e^{-\gamma\zeta}(e^{\tau} - 1)\right]^{-1} \tag{8}$$

$$[M_N](\zeta,\tau) = \exp\left\{-\frac{2\beta}{(1-e^{-\gamma\zeta})^{1/2}}\arctan\left[\frac{(e^{\gamma\zeta}-1)^{1/2}(e^{\tau/2}-1)}{e^{\gamma\zeta}-1+e^{\tau/2}}\right]\right\} \tag{9}$$

where $[A_N]$ and $[M_N]$ are the normalized initiator and monomer concentration, respectively. The solutions are expressed in terms of the non dimension variables:

$$\zeta = z/D \tag{10}$$

$$\tau = \phi I_0 \alpha_A t \tag{11}$$

where D is the thickness of the polymeric material.

The following parameters are also defined:

$$\beta = k_p\left[\frac{f[A]_0}{\phi\alpha_A I_0 k_t}\right]^{1/2} \tag{12}$$

$$\gamma = \alpha_A [A]_0 D \tag{13}$$

Fig. 1 shows the monomer conversion (1-[M_N]) as a function of the dimensionless variable ζ for four values of the parameter γ. The value of β was of 1^{20} and the dimensionless time τ was found imposing that the average concentration of photoinitiator in the material is $[\overline{A}_N] = 0.75$, the average concentration of photoinitiator defined as:

$$[\overline{A}_N] = \int_0^1 [A_N(\zeta, \tau)] d\zeta \tag{14}$$

the average monomer concentration is also defined as:

$$[\overline{M}_N] = \int_0^1 [\overline{M}_N(\zeta, \tau)] d\zeta \tag{15}$$

From Fig. 1 it can be seen that there is a depth attenuation of monomer conversion which is increased with the value of γ. In Fig. 2 the monomer conversion is represented as a function of ζ for an average concentration of photoiniatior of $[\overline{A}_N] = 0.5$. The same effects described in Fig. 1 can be seen, but in this case, for a higher initiator consumption, the values of monomer consumption are increased.

Fig. 3 represents the average monomer consumption as a function of τ for four different values of γ and a value of β=1, where it can be seen that γ controls the rate of monomer conversion and, therefore the rate of polymerization. The higher the value of γ the higher the rate of polymerization.

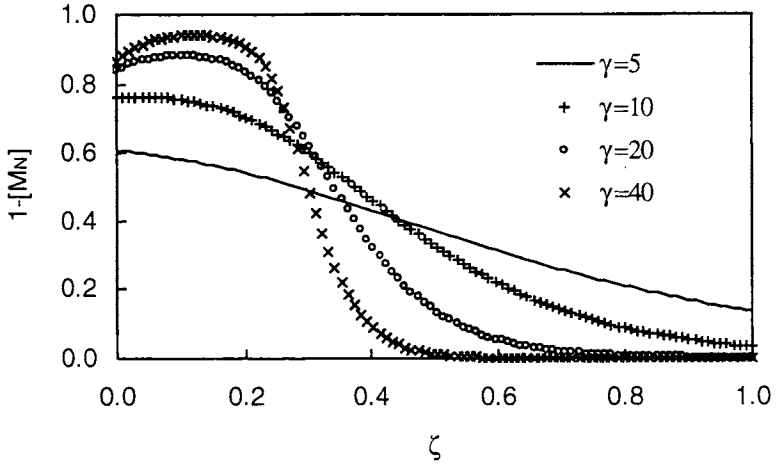

Fig 1. Monomer conversion as a function of the normalized depth for different values of γ. β=1 in the theoretical simulations and $[\overline{A}_N] = 0.75$

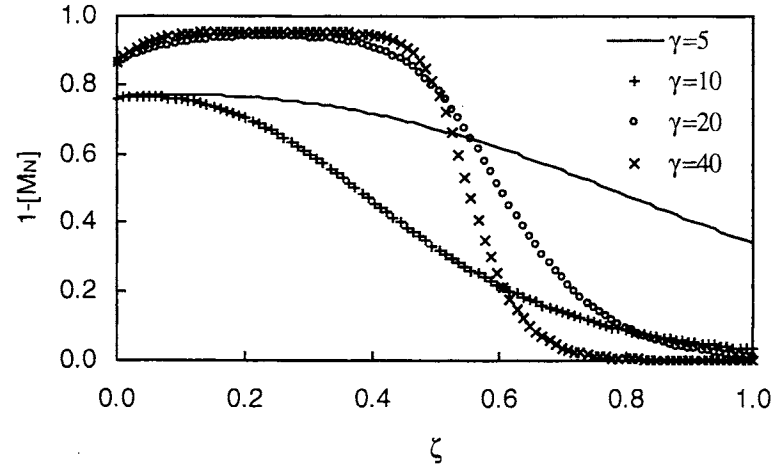

Fig 2. Monomer conversion as a function of the normalized depth for different values of γ. β=1 in the theoretical simulations and $[\bar{A}_N]=0.5$.

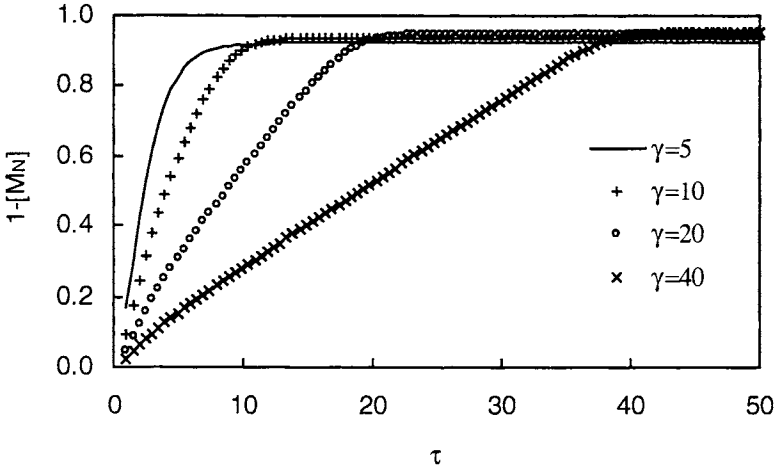

Fig 3. Average monomer conversion as a function of the normalized time for different values of γ. β=1 in the theoretical simulations.

The main conclusion that should be extracted is that photopolymerization mechanisms imply an attenuation of the monomer and polymer concentration profiles through the depth of the material. This attenuation must be taken into account in order to calculate the efficiencies of the different orders that propagate inside the grating. In next section we will explain how this attenuation influences on the efficiency curves of the different orders.

3. RIGOROUS COUPLED WAVE METHOD FOR PERIODIC ATTENUATED PROFILES

In this section we explain how the behavior of the different diffracted orders propagating inside a transmission diffraction grating with an attenuated refractive index profile can be derived using the formalism of ref. 20.
For an unslanted grating the profile of the dielectric permittivity can be expressed in the form:

$$\varepsilon(x,z) = \sum_h \varepsilon_h(z) \exp[jhKx] \tag{16}$$

K is the modulus of the grating vector, which is related to the period of the interference fringes, Λ, as follows:

$$K = 2\pi/\Lambda \tag{17}$$

$\varepsilon_h(z)$ are the harmonics of the dielectric permittivity that, assuming attenuation, can be expressed as:

$$\varepsilon_h(z) = \varepsilon_{h,0} \exp[-\alpha z] \tag{18}$$

where $\varepsilon_{h,0}$ are the initial values (at z=0) of the harmonic components of the dielectric permittivity.

The method to obtain the efficiencies of the orders that propagate in the hologram consists in dividing the periodic structure in G different sub-gratings of thickness d_g each and apply the algorithm of ref. 19. to each sub-grating. This method is explained in ref. 18.

Each sub-grating will be supposed to have a periodic dielectric permittivity of the form:

$$\varepsilon_g(x) = \sum_h \varepsilon_{g,h} \exp[jhKx] \tag{19}$$

$\varepsilon_{g,h}$ is the h^{th} Fourier component of the relative permittivity in the grating region g, which can be expressed as:

$$\varepsilon_{g,h} = \varepsilon_{0,h} \exp[-\alpha \sum_{g'=1}^{g} d_{g'}] \tag{20}$$

In order to obtain numerical results for the angular responses of the different diffracted orders that propagate in holograms with attenuated profiles a theoretical diffraction grating with a spatial frequency of 500 lines/mm and 80 μm thick was studied. The average refractive indices chosen for the theoretical simulations were: n_a=1, n_p=1.59 and n_v=1.53 for air, polymer and glass, respectively and the number of orders retained in the calculations was of 21: 0, ±1, ±2, ±3, ...

We assumed that the grating had a refractive index profile of the form:

$$n(z) = n_0 + n_1(z)\cos[Kx] + n_2(z)\cos[2Kx] + n_3(z)\cos[3Kx] \tag{21}$$

where:

$$n_i(z) = n_{i,0} \exp(-\alpha z) \qquad \text{for i=1,2,3} \tag{22}$$

Fig. 4 shows the efficiency of the first order as a function of the angle in air for different values of α, and for an unslanted transmission diffraction grating of spatial frequency 500 lines/mm. The efficiency is shown in logarithm scale and the angular response is centred at the first on Bragg replay angular condition. The values used in the theoretical calculations were a thickness of 80 μm and the amplitudes of the three harmonic components of the refractive index were:$n_{1,0}$=0.004, $n_{2,0}$=$n_{1,0}$/8, $n_{3,0}$=$n_{1,0}$/20. These values were assumed for all the theoretical diffraction gratings studied presented here. It is clear that the effect of an attenuated profile is to decrease the efficiency of the first order.

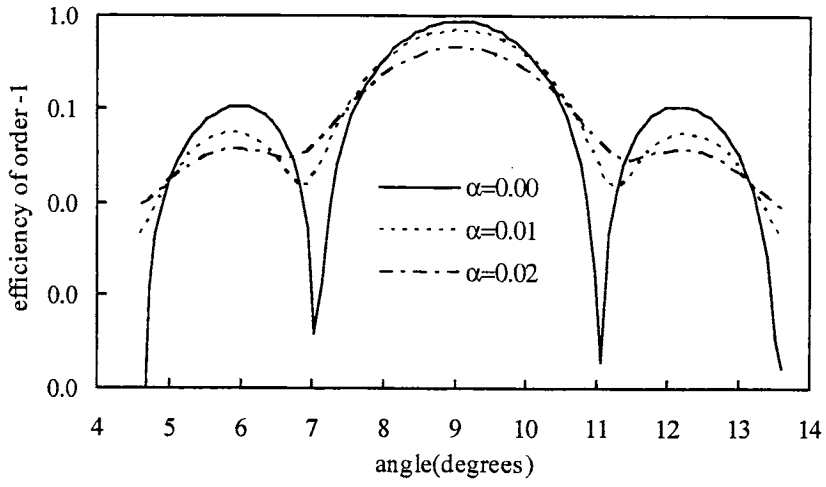

Fig. 4. Efficiency of order -1, as a function of the angle, centered at first on Bragg angular replay condition for different values of the attenuation constant α: 0.00 μm^{-1}, 0.01 μm^{-1}, 0.02 μm^{-1}, for a spatial frequency of 500 lines/mm. The number of layers was of 50.

Figs. 5 and 6 show the efficiencies of the second and first order, respectively, as a function of the angle in air for different values of α and for a transmission diffraction grating with a spatial frequency of 500 lines/mm. The angular response is centred at the second Bragg angular replay condition. Again, the effect of the attenuation in the different harmonic components of the refractive index is to smooth the off Bragg curve.

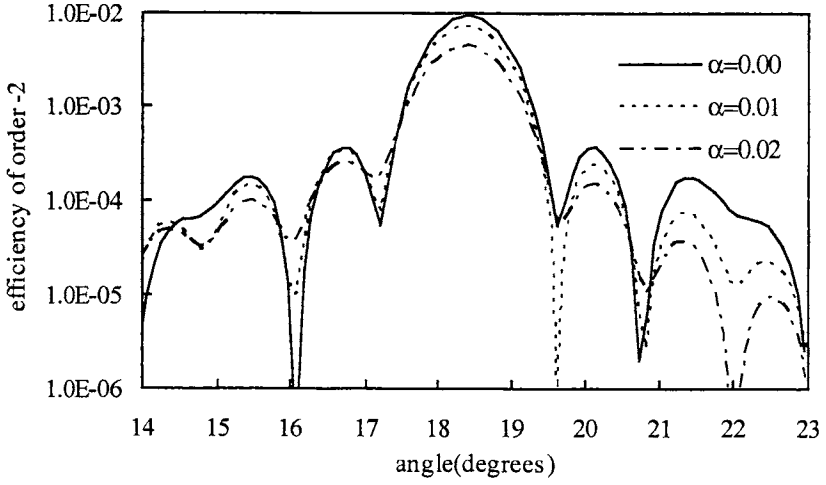

Fig. 5. Efficiency of order -2, as a function of the angle, centered at second on Bragg angular replay condition for different values of the attenuation constant α: 0.00 μm^{-1}, 0.01 μm^{-1}, 0.02 μm^{-1}, for a spatial frequency of 500 lines/mm. The number of layers was of 50.

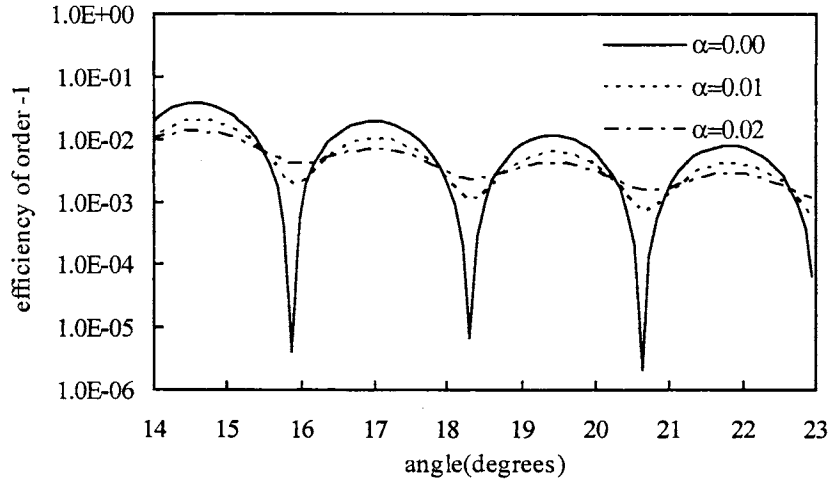

Fig. 6. Efficiency of order -1, as a function of the angle, centered at second on Bragg angular replay condition for different values of the attenuation constant α: 0.00 μm^{-1}, 0.01 μm^{-1}, 0.02 μm^{-1}, for a spatial frequency of 500 lines/mm. The number of layers was of 50.

Finally Figs. 7 and 8 show the efficiency of the third and first order, respectively, as a function of the angle in air for different values of α and for a transmission diffraction grating with a spatial frequency of 500 lines/mm. The angular response is centred at the third Bragg angular replay condition. Clearly the same effects observed in previous cases, is observed. Nonetheless, there exist a higher number of lateral lobes to the main one for the efficiency of the third order if compared to the efficiency of the first order in Fig. 4. This is due to the fact that the angular selectivity is reduced whenever the angular responses are centred at higher Bragg angular replay conditions.

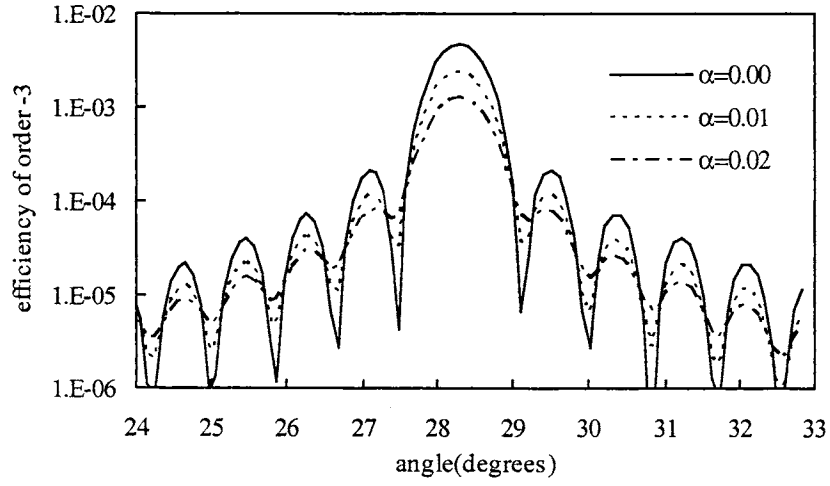

Fig. 7. Efficiency of order -3, as a function of the angle, centered at third on Bragg angular replay condition for different values of the attenuation constant α: 0.00 μm^{-1}, 0.01 μm^{-1}, 0.02 μm^{-1}, for a spatial frequency of 500 lines/mm. The number of layers was of 50.

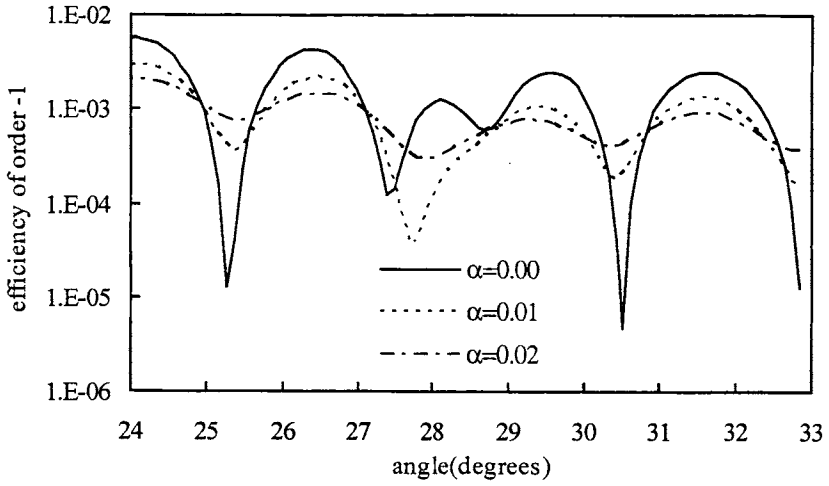

Fig. 8. Efficiency of order -1, as a function of the angle, centered at third on Bragg angular replay condition for different values of the attenuation constant α: 0.00 μm^{-1}, 0.01 μm^{-1}, 0.02 μm^{-1}, for a spatial frequency of 500 lines/mm. The number of layers was of 50.

In order to compare the theoretical simulations with experimental results unslanted diffraction gratings of 540 lines/mm were recorded in PVA/acrylamide photopolymer material using an Argon laser of wavelength 514 nm. To prepare the material a method similar to that described in other papers was used[21-24].

Fig. 9 presents the efficiency of the second order as a function of the reconstruction angle for a diffraction gratings recorded with a spatial frequency of 545 lines/mm. The angular response was centered at the second on Bragg replay angular condition. It can be seen that there is good agreement between the theory and the experiment. The smoothing of the off-Bragg commented is observed for the efficiency of the second order.

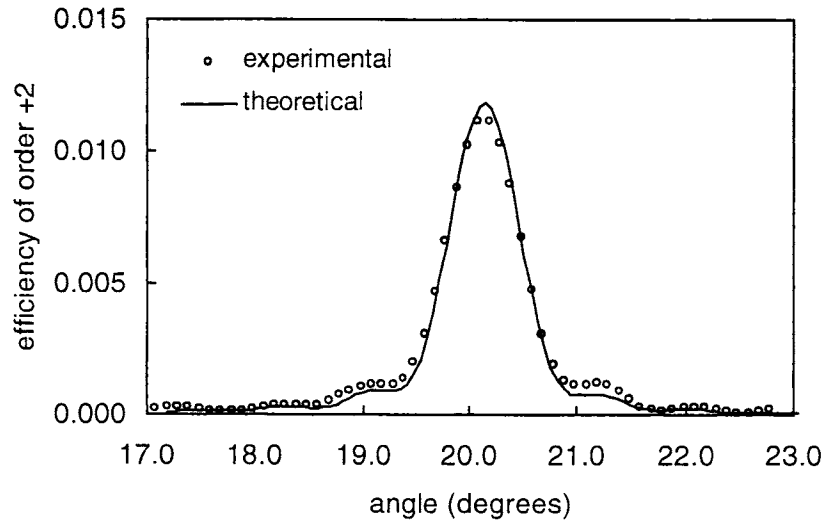

Fig. 9. Efficiency of order -2 as a function of the angle, centered at first on Bragg angular replay condition a transmission grating recorded on PVA/Acrylamide photopolymer with a spatial frequency of 545 lines/mm and a thickness of 117 μm. The number of layers was of 50.

4. CONCLUSIONS

It has been demonstrated that photopolymerization mechanisms yield to attenuation in depth of monomer and polymer concentrations. As a result an attenuation of the refractive index is present in diffraction gratings recorded in photopolymer materials. In order to take into account this effect an algorithm based on the RCW formalism is proposed, and simulations of the efficiency for the different orders that propagate in the hologram have been presented for a transmission diffraction grating of 500 lines/mm. In general the smoothing in the off-Bragg response curves for the first order has also found in the higher orders. Finally, the experimental data presented for the angular responses the second order centered at second on Bragg angular replay condition, demonstrated that an attenuated refractive index profile is stored in volume gratings recorded in PVA/Acrylamide photopolymer materials.

ACKNOWLEDEGMENTS

This work was supported by the Ministerio de Ciencia y Tecnología, CICYT, Spain, under project MAT2000-1361-C04-04. 04.

REFERENCES

1. R. A. Lessard and G. Manivannan, Eds., "Selected Papers on Photopolymers", **MS 114**, SPIE Optical Engineering Press, Belligham, Washington, 1996.
2. D.J. Lougnot, "Self-processing photopolymer materials for holographic recording", *Crit. Rev. Opt. Sci. Technol.*, **CR63**, 190-213, 1996.
3. Coufal H J, Psaltis D, *Holographic data storage*, Sincerbox G T, 2000.
4. R. R. Adhami, D. J. Lanteigne, D. A. Gregory, "Photopolymer hologram formation theory", *Microwave and Optical Technology Letters*, **4**, 106-109, 1991.
5. G. Zhao, P. Mouroulis, "Diffusion model of hologram formation in dry photopolymer materials", *Journal of Modern Optics*, **41**, 1929-1939, 1994.
6. S. Piazzolla, B. Jenkins, "Holographic grating formation in photopolymers", *Optics Letters*, **21**, 1075-1077, 1996.
7. V. L. Colvin, R. G. Larson, A. L. Harris, M. L. Schilling, "Quantitative model of volume hologram formation in photopolymers", *Journal of Applied Physics*, **81**, 5913-5923, 1997.
8. I. Aubrecht, M. Miler, I. Koudela, "Recording of holographic diffraction gratings in photopolymers: theoretical modelling and real-time monitoring of grating growth", *Journal of Modern Optics*, **45**, 1465-1477, 1998.
9. J. H. Kwon, H. C. Chang and K. C. Woo, "Analysis of temporal behavior of beams diffracted by volume gratings formed in photopolymers", *Journal of Optical Society of America B*, **16**, 1651-1657, 1999.
10. G. M. Karpov, V. V. Obukhovsky, T. N. Smirnova, V. V. Lemeshko, "Spatial transfer of matter as a method of holographic recording in photoformers", *Optics Communications*, **174**, 391-404, 2000.
11. J. T. Sheridan, J. R. Lawrence, "Non-local response diffusion model of holographic recording in photopolymer", *Journal of Optical Society of America B* , **17**, 1108-1114, 2000.
12. J. T. Sheridan, M. Downey, F. T. O'Neill, "Diffusion based model of holographic grating formation in photopolymers: Generalised non-local material responses", *Journal of Optics A: Pure and Applied Optics*, **3**, 477-488, 2001.
13. J. R. Lawrence, F. T. O'Neill, J. T. Sheridan, "Adjusted intensity non-local diffusion model of photopolymer grating formation," *Journal of Optical Society of America B*, **19**, 621-629, 2002.
14. S. Wu and E. N. Glytsis, "Holographic grating formation in photopolymers: analysis and experimental results based on a nonlocal diffusion model and rigorous coupled-wave analysis", *Journal of Optical Society of America B*, **20**, 1177-1188, 2003.
15. C. Neipp, S. Gallego, M. Ortuño, A. Márquez, M. Álvarez, A. Beléndez and I. Pascual, "Fist harmonic diffusion based model applied to PVA/acrylamide based photopolymer", *Journal of Optical Society of America B*, **20**(10), 2052-2060, 2003.
16. S. Blaya, L. Carretero, R. Mallavia, A. Fimia, and R. F. Madrigal, "Holography as a technique for the study of photopolymerization kinetics in dry polymeric films with a nonlinear response", *Applied Optics*, **38**, 955-962, 1999.

17. S. Blaya, L. Carretero, R. F. Madrigal and A. Fimia, "holographic study of chain length in photopolymerizale compositions", *Applied Physics B*, **74**, 243-251, 2002.
18. C. Neipp, J. T. Sheridan, S. Gallego, M. Ortuño, A. Márquez, I. Pascual and A. Beléndez, "Effect of a depth attenuated refractive index profile in the angular responses of the efficiency of higher orders in volume gratings recorded in a PVA/Acrylamide photopolymer", *Optics Communications*, accepted for publication.
19. M. G. Moharam, E. B. Grann, D. A. Pommet and T. K. Gaylord, " Formulation for stable and efficient implementation of the rigurous coupled-wave analysis of binary gratings", *Journal of Optical Society of America A*, **12**, 1068-1076, 1995.
20. G. Terrones, A. J. Pearlstein, "Effects of kinetics and optical attenuation on the completeness, uniformity, and dynamics of monomer conversion in free-radical photpolymerization", *Macromolecules*, **34**, 8894-8906, 2001.
21. S. Blaya, L. Carretero, R. Mallavia, A. Fimia, M Ulibarrena and D. Levy, "Optimization of an acrylamide-based dry film used for holographic recording", *Applied Optics*, **37**, 7604, 1998.
22. C. García, A. Fimia, I. Pascual, "Diffraction efficiency and signal-to-noise ratio of diffuse-object holograms in real time in polyvinyl alcohol photopolymers", *Applied Optics* , **38**, 5548 1999.
23. C. García, A. Fimia, I. Pascual, "Holographic behavior of a photopolymer at high thicknesses and high monomer concentrations: mechanism of polymerization", *Applied Physics B*, **72**, 311-316, 2001.
24. S. Gallego, M. Ortuño, C. Neipp, C. García, A. Beléndez and I. Pascual, "Temporal evolution of the angular response of a holographic diffraction grating in PVA/acrylamide photopolymer", *Optics Express*, **11**, 181-190, 2003.